FAULT LOCALIZATION FOR INDEPENDENT METERING SYSTEMS BY MODEL-BASED FAULT DETECTION

Eric Fischer[1]*, Benjamin Beck[1], Jürgen Weber[1]

[1]*Institute of Mechatronic Engineering, Chair of Fluid Mechatronic Systems (Fluidtronics), Technische Universität Dresden, Helmholtzstrasse 7a, 01069 Dresden*

* Corresponding author: Tel.: +49 351 463-33553; E-mail address: eric.fischer1@tu-dresden.de

ABSTRACT

This paper deals with fault localization for a mobile hydraulic system with independent metering, but it is also applicable to other hydraulic systems. The basis for this contribution is a model-based fault detection, which generates multiple symptom patterns for various component failures using a set of parity equations (see previous publications from the authors). The symptom patterns are evaluated through different classification methods such as geometric, statistical, and artificial intelligence methods. The evaluation focuses on simple approaches that are applicable in practice. Taking into account the limitations of mobile systems, different operating points, and a variety of fault scenarios, a correct fault localization of up to 92% of detected faults is possible. After locating faults correctly, IM systems enable a range of reconfiguration modes to keep the machine's functionality and therefore rise the availability. Laboratory demonstrator tests confirm the simulation-based outcomes.

Keywords: fault localization, model-based fault detection, independent metering, safety, reliability

1. INTRODUCTION

Systems with independent control edges offer high energy efficiency and great structural flexibility. To fully exploit these benefits, electrohydraulic drive systems and sensor technology are required. Despite the ongoing digitalization and automation of machines, there are only a few market-ready implementations of independent metering (IM) systems such as [1] and [2]. Possible reasons for this are the increased system complexity of IM systems in combination with extensive control algorithms, software architectures and safety aspects.

Previous work shows that IM systems are capable of meeting high safety requirements if the required diagnostic coverage is provided [3]. One possibility to achieve the required diagnostic coverage is a model-based fault detection, using parity equations. The implementation of such a reliable fault detection was shown in [4]. The increased system complexity creates the opportunity to use a set of eleven different parity equations with individual boundaries. These customized balance limits lead to varied sensitivity of the parity equations under diverse fault conditions. The resulting symptom pattern provides the basis of the investigated fault localization presented here.

Starting with the introduction of the object of study, basic approaches for fault detection are derived and their practical validation is presented in this paper. While maintaining knowledge-based (model-based) approaches, different methods for fault localization are introduced and implemented. The accuracy of their localization is compared. Test bench measurements confirm the effectiveness of the localization algorithms. The well-functioning fault localization allows partial compensation of faulty components through various reconfiguration modes - structural measures or control interventions to provide defined machine movement in case of failure - thus increasing availability.

2. SUBJECT OF INVESTIGATION

Subject of investigation is the independent metering (IM) system of the excavator test rig at the research centre. The system includes two IM sections, each consisting of two pilot-operated 2/2 proportional valves (see **Figure 1**, $V_{prop,A}$, $V_{prop,B}$) and four 2/2 switching valves ($V_{sv,AP}$, $V_{sv,AT}$, $V_{sv,BP}$, $V_{sv,BT}$). These IM sections are responsible for controlling the boom and stick cylinder of a compact excavator implement. The proportional valves regulate the flow rate and cylinder pressure according to the methods described in [5], while the switching valves determine the operation mode of the IM structure. The test rig enables extensive sensory monitoring. Sensors measure the cylinder velocities, the spool positions of the proportional valves and all pressures in the cylinder chambers and between the valves.

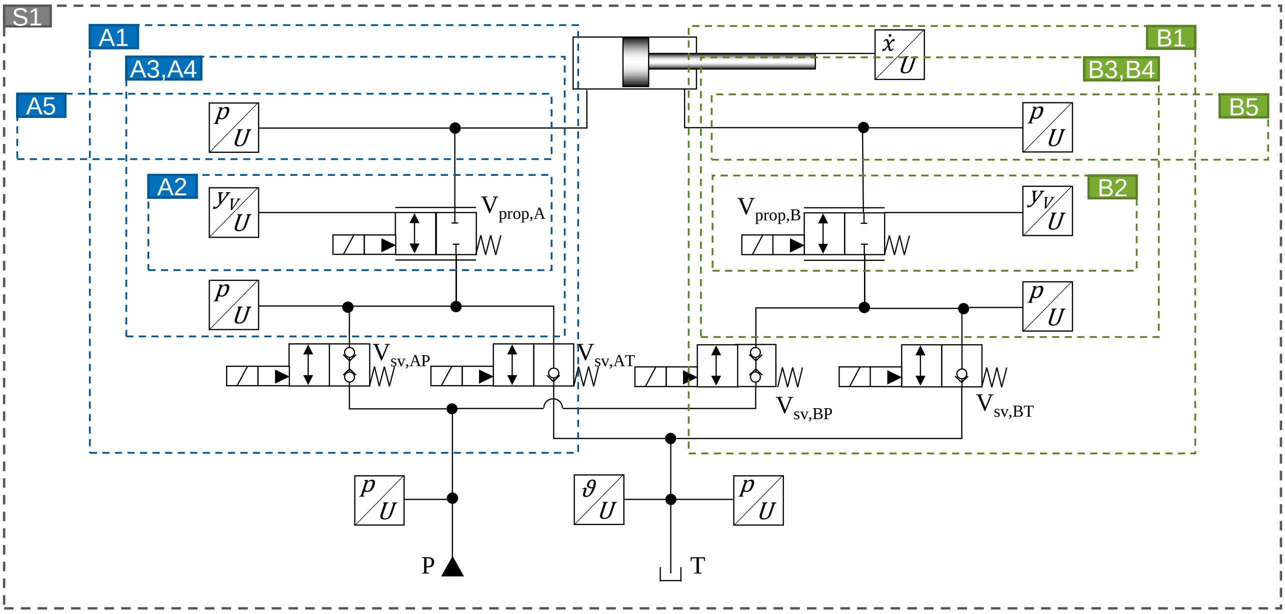

Figure 1: Design of the investigated independent metering system.

In addition to the physical test bench, a validated software-in-the-loop (SIL) environment is used for the development of the fault detection and localization algorithms. A comprehensive variant study enables the consideration of a large number of components that may cause errors, as well as different error characteristics and operating points. This takes into account the system complexity on the one hand and the operator-guided control of mobile machines on the other. The SIL environment has certain limitations that are typical in software development for mobile machinery, e.g. low computing capacities and restricted task times of the control unit. In total, 7 operating points with 542 error scenarios each form the basis of the investigation [4].

3. MODELL-BASED FAULT DETECTION

The test rig's vast sensory equipment enables the calculation of several parity equations. The aim of these equations is to generate residuals through the comparison of measured and calculated output variables. To calculate the theoretical values, practical model descriptions are used for fluid behavior, valve dynamics, pressure build-up in hydraulic capacities, and volume flow through the valves. Combined with sensor data and control values, this results in two parity equations for the valve positions (A2, B2, see Figure 1), eight for the cylinder velocities (A1 to A5, B1 to B5, except A2, B2) and one for the volume flow to be supplied by the pump (S1). The majority of parity equations have fixed, very local balance limits and are entirely defined by the associated measured and calculated values. These equations are therefore also called local parity equations. Equations A5, B5 and S1 contain set points from the machine control, which depend on the state of the overall system. Thus, these equations are termed global parity equations.

A threshold check controls the resulting residuals. Because the modeling is as simple and practical as possible, deviations between calculated and measured values are inevitable. If the residuals exceed the acceptable threshold for a prolonged duration of time, the mathematical model deviates significantly from the actual system process. In this case, a faulty state is to be assumed and an error symptom is generated. This symptom is used for error detection.

As shown in [4], model-based fault detection generates at least one symptom for up to 70% of the imprinted fault cases, dependent on the operating point and as displayed in **Figure 2**. However, a significant percentage of the errors remain undetected. To evaluate the effectiveness of fault detection, it is necessary to assess the potential danger of any detected or undetected errors. For this purpose, it is suitable to consider the position deviations of the cylinder due to the error in comparison to the fault-free state. The histograms illustrate these position deviations Δx_{cyl} 2 seconds after the fault occurs. In the case of an undetected fault (symptomless), the movement of the cylinder generally deviates only slightly from its fault-free state. However, if a fault is detected, serious and dangerous changes in movement may occur. The undetected faults therefore do not lead to a dangerous situation, while all dangerous faults are detected. This leads to Diagnostic Coverage values of up to DCavg=99 % for the safety evaluation process.

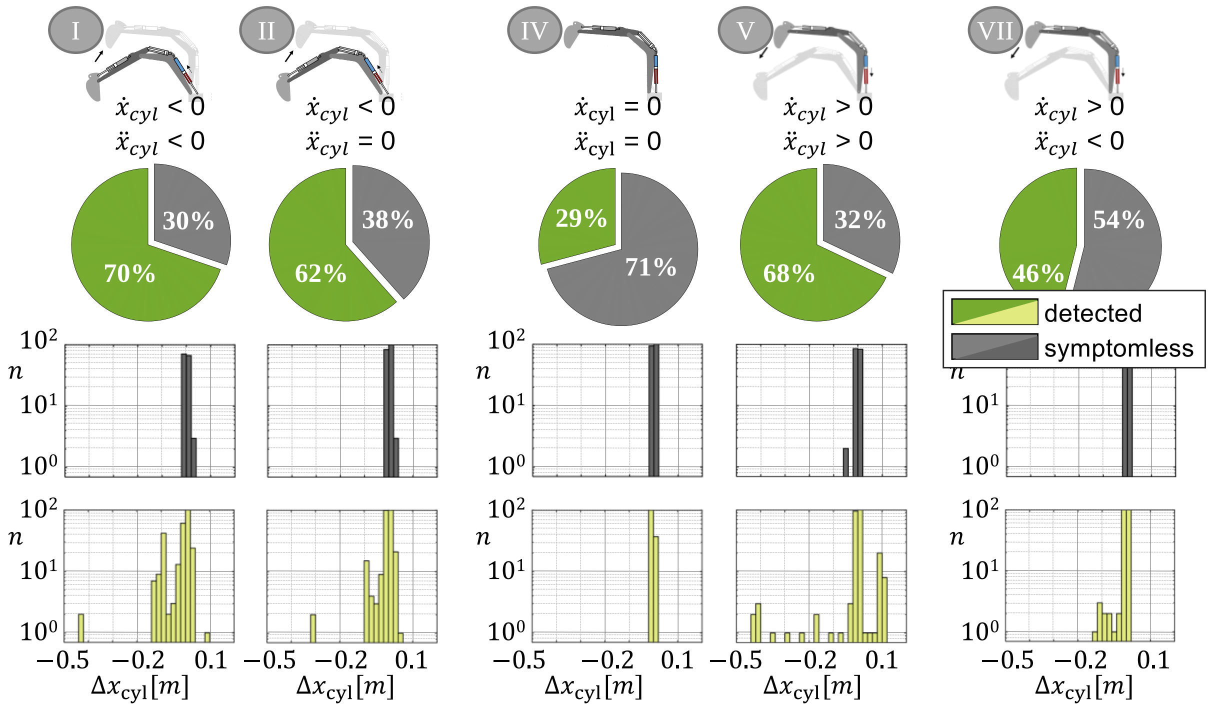

Figure 2: Amount of detected faults and their impact on the cylinder position for different operating points.

To confirm the results of the simulative variant study, various fault scenarios are reproduced on the test rig. For this purpose, the detection algorithms are transferred to the test rig controller (HY-TTC 580). To ensure consistency, the test rig demonstrator autonomously executes the reference cycle of the simulation study. A Fault Insertion Unit enables the time-controlled emulation of component faults so that the practical tests match the simulated conditions as closely as possible.

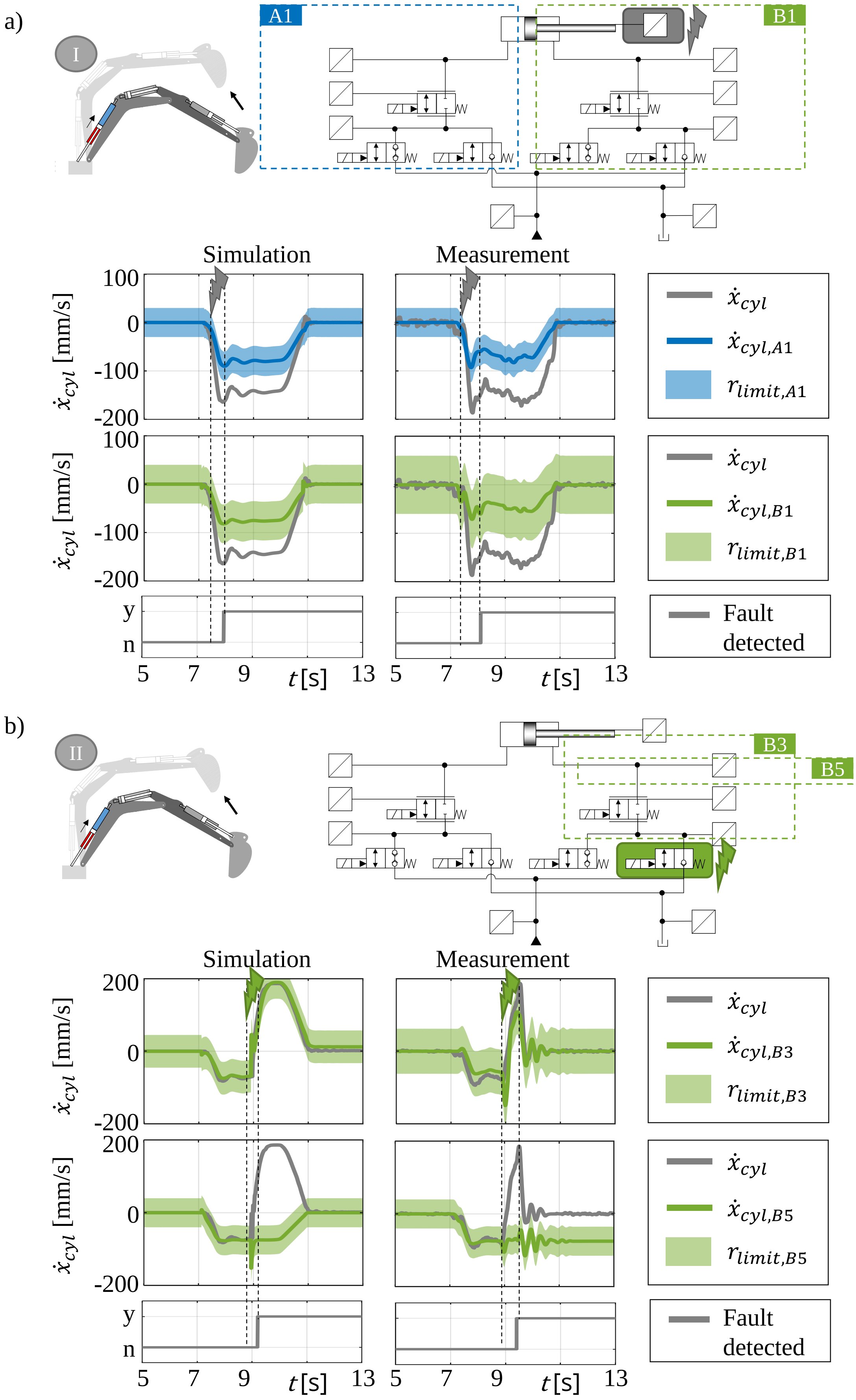

Figure 3: a) Error of the cylinder velocity sensor at operating point I,
b) Error of the switching valve $V_{sv,BT}$ at operating point II.

Figure 3 shows the comparison of simulated and measured behavior for two fault scenarios. The fault detection of two parity equations for a malfunctioning cylinder velocity sensor is displayed in Figure 3 a). The absolute measured value is greater than the actual velocity. The parity equations A1 and B1 calculate a velocity the cylinder should achieve within their balance limit, the corresponding valve section and cylinder chamber. The measured velocity signal acts as a reference value for both equations. Due to inaccuracies in the model and measurement deviations, the calculated velocity is subject to an uncertainty (r_{limit}). When an error occurs, the measured value exceeds the acceptable tolerance range. If the deviation remains over for a certain period of time, the fault detection identifies the presence of a faulty condition. Since the tolerance range was exceeded by both A1 and B1, both parity equations produce an error symptom. Simulation and measurement match qualitatively and quantitatively very well.

Another example is shown in Figure 3 b). During the lifting of the boom, the valve $V_{sv,BT}$ is opened in a faulty manner. As a result, the load-holding cylinder side is relieved against the reservoir and the attachment drops to the ground. The faulty valve is outside the balance limits of the local parity equation B3, which is mainly determined by valve flow characteristic of $V_{prop,B}$. Therefore, there is no error in the scope of the parity equation. The figure clearly shows that equation B3 accurately computes the motion resulting from the error. The global parity equation B5, on the other hand, detects the fault immediately after it occurs. Only B5, which uses the set volume flow through valve $V_{prop,B}$ for calculation, produces an error symptom. Again, measurement and simulation match very well. In the absence of any error reaction measure, the boom cylinder reaches its end position in the simulation while its motion is constrained by the floor during the laboratory test.

The test rig results on the one hand validate the results of the variant study and on the other hand show the selective behavior of the generated symptoms in case of different faults. This is a prerequisite for a proper fault localization.

4. DEVELOPMENT OF FAULT LOCALIZATION

The aim of fault localization is the identification (detection) of a faulty component. This first requires the detection of a faulty state. As seen before, the fault detection method utilizing eleven parity equations and the resulting symptoms provides a solid foundation for achieving this goal. In the following, four different approaches for fault localization will be presented. These work in detail…

1. …on the basis of complete feature matching,
2. …using decision or fault trees,
3. …according to the Manhattan distance or
4. …via learning vector quantization.

As shown, the parity equations have different error sensitivities due to their different balance limits. According to these limits, there are expectations regarding the symptom patterns that occur with different faults. **Table 1** illustrates the expected symptom patterns for cylinder retraction.

Table 1: Expected symptom pattern for different fault classes during cylinder retraction

		Symptom generating parity equation							
Fault description, Error of…	Fault class	A1	A2	A3	A4	B1	B2	B3	B4
the proportional valve $V_{prop,A}$	i-p-A	x			x				
the proportional valve $V_{prop,B}$	i-p-B					x			x
the position sensor on valve $V_{prop,A}$	y-p-A-sens		x	x					
the position sensor on valve $V_{prop,B}$	y-p-B-sens						x	x	

the switching valves on the piston side or of the tank pressure sensor (no distinction possible)	pT,AT,AP	x							
the switching valves on the rod side or of the system pressure sensor (no distinction possible)	p0,BT,BP					x			
the cylinder pressure sensor on the piston side	p-A-sens	x		x	x				
the cylinder pressure sensor on the rod side	p-B-sens					x		x	x
the pressure sensor between the switching valves and the proportional valve (piston side)	p-α-sens			x	x				
similar to fault class p-α-sens, but for rod side	p-β-sens							x	x
the cylinder velocity sensor	v-cyl-sens	x		x	x	x		x	x

The first three approaches take advantage of this knowledge. However, as described above, the global parity equations do not have the required selectivity. Consequently, the localisation of these methods relies entirely on local parity equations. For this reason, only the local symptom-generating parity equations are listed in Table 1.

4.1. Fault localization based on the complete feature matching

As shown in Table 1 faults with the same symptom pattern were grouped into a fault class (e.g.: pT,AT,AP). The current set of parity equations cannot distinguish between them. To differentiate between these faults, an expanded equation base is required. For example, Richter [6] and Kramer [7] present a way to directly monitor the state of the switching valves. Each fault class has a unique symptom pattern. Therefore, if one of these individual patterns appears due to a faulty condition, it can be assumed that the component fault underlying the fault class is responsible. This constitutes a basic form of fault localization. All detected fault cases are analyzed for complete feature matching, based on the variant study. A confusion matrix presents the result of the fault localization. The matrix compares the actual error class (true class) with the class classified by the algorithm (predicted class). The matrix's numerical values indicate the frequency of each classification. On the matrix diagonal, correctly classified error cases can be identified.

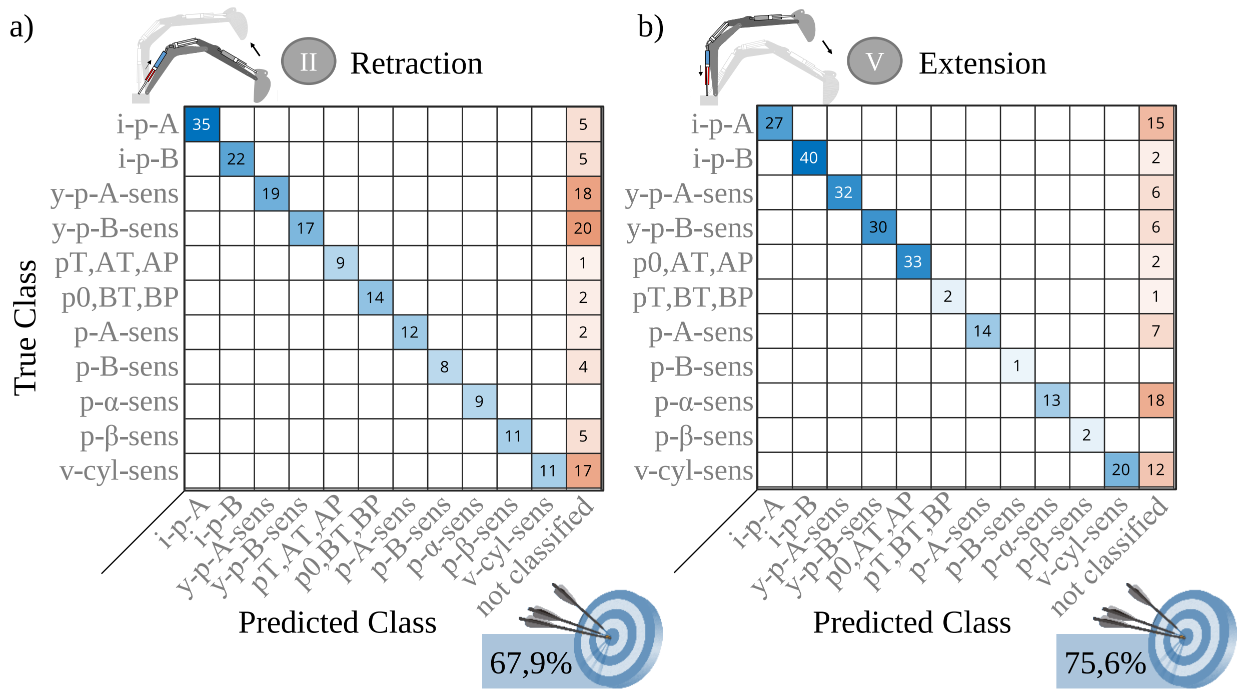

Figure 4: Confusion matrix for a) operating point II and b) operating point V with localization by means of complete feature matching.

As expected, classification based on full feature expression does not lead to any mislocalizations (refer to **Figure 4**). Nevertheless, the overall localization accuracy is only about 68% and 75%. In approximately 30% of the analyzed detected faults, not all parity equations produce an expected symptom. This leads to the absence of a complete symptom pattern, making a fault case classification impossible (not classified faults).

4.2. Fault localization using fault trees

Since a complete symptom pattern is a major limitation for fault localization, other approaches are being considered. One of these is the utilisation of fault trees. According to Isermann, error trees belong to statistical approaches [8]. This approach uses a series of hierarchical decisions to identify possible fault causes. Starting from a root decision node, the presence or absence of particular symptoms is checked. Depending on the result, the following decision node is then reached. At the end of each decision path are the individual fault classes. A complete feature expression is not required, but it improves localization quality. There are various methods to create a fault tree. One method is to train the fault tree using the existing data set (variant simulation). An other method is to use the expected symptoms (refer to Table 1) to generate an analytical fault tree. The analytical approach allows the inclusion of "expert knowledge", such as the combination of criteria as well as the prioritization of decision nodes. **Figure 5** illustrates the result of the classification based on an analytical decision tree. The confusion matrices demonstrate that improved error localization is achievable at both operating points, with an increase in overall localization accuracy of between 12 to 16%. The fault tree assigns a possible fault class to all detected faults. However, it can result in some incorrectly localized faults. For example, 16 out of 28 faults of the cylinder velocity sensor are localized correctly in operating point II.

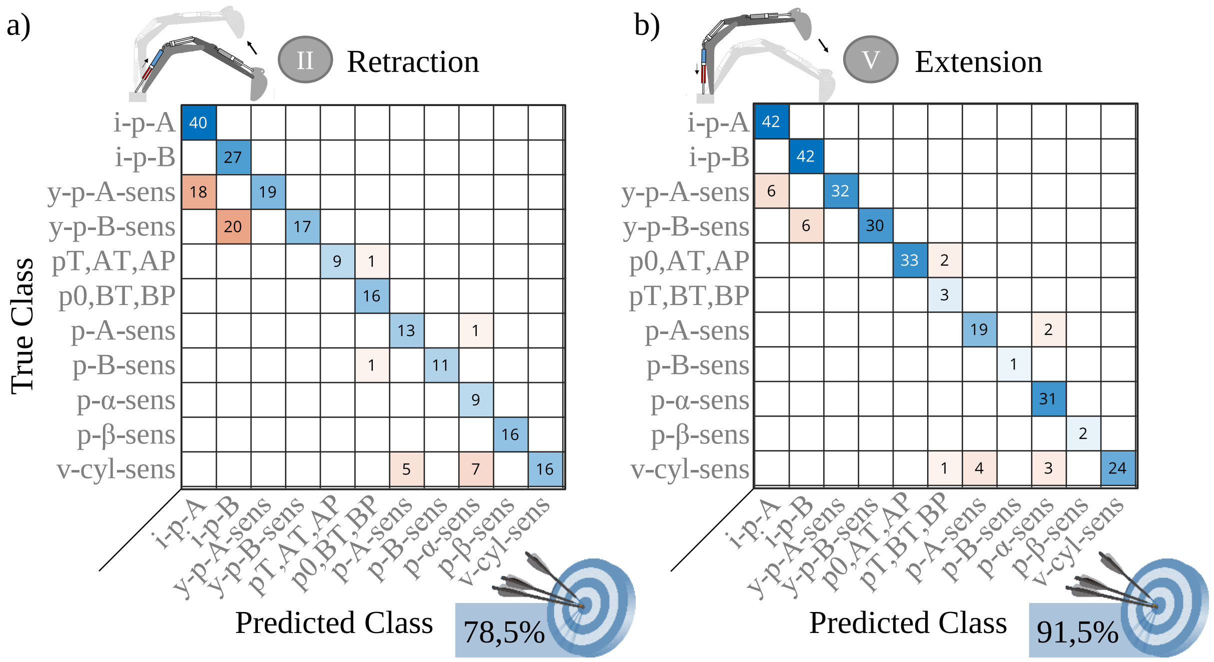

Figure 5: Confusion matrix for a) operating point II and b) operating point V with localization by means of fault tree.

The hierarchical structure of a fault tree is a drawback as it strongly prioritizes selected symptoms, making the sequence of decisions critical. Correct localization becomes challenging when a highly prioritized expected symptom is absent.

4.3. Fault localization according to the Manhattan distance (City-block-distance)

The Manhattan distance is a geometric classification method, where the assignment of individual fault classes is based on geometric distance [8]. Each class has a prototype that is specific to its class, whose symptom expression is characteristic and representative for this particular class. In this case, the prototype aligns with the expected symptom pattern. The closer the distance between a prototype and an object to be classified, the higher the likelihood of it belonging to the corresponding class [9].

The term Manhattan (or city block) distance originates from the fact that in urban areas, distance between two points can only be determined along specific coordinate directions (e.g. streets, lifts). The Euclidean distance ("as the crow flies") is not suitable for this. By interpreting the features of individual parity equations as directions (A1, A2, ..., B4) and their corresponding symptoms (0,1) as distance, this method can be used for fault localization. Neither a fully developed symptom pattern nor a hierarchical structuring of the individual symptoms is necessary. In general, distance measures offer the possibility of weighting diverse "directions" differently. However, since the equality of all symptoms is an advantage over fault trees, this possibility is not used. Nevertheless, a suitable weighting is purposeful. By choosing robust threshold values for fault detection, the occurrence of unexpected symptoms is hardly possible, while the absence of an expected symptom is probable. For this reason, the matching of existing symptoms is weighted more heavily than their absence.

The geometric classification achieves a very good overall localisation accuracy above 90% for both operating points, as shown in **Figure 6**. Due to the possibility of several prototypes having the smallest distance value, a single fault scenario can be assigned to multiple classes. The sum of all classifications can therefore exceed the sum of the investigated scenarios. If other potential causes are also assigned to a fault in addition to the correct fault class, it is still considered a correctly localized fault, since focused troubleshooting in practical use is simplified.

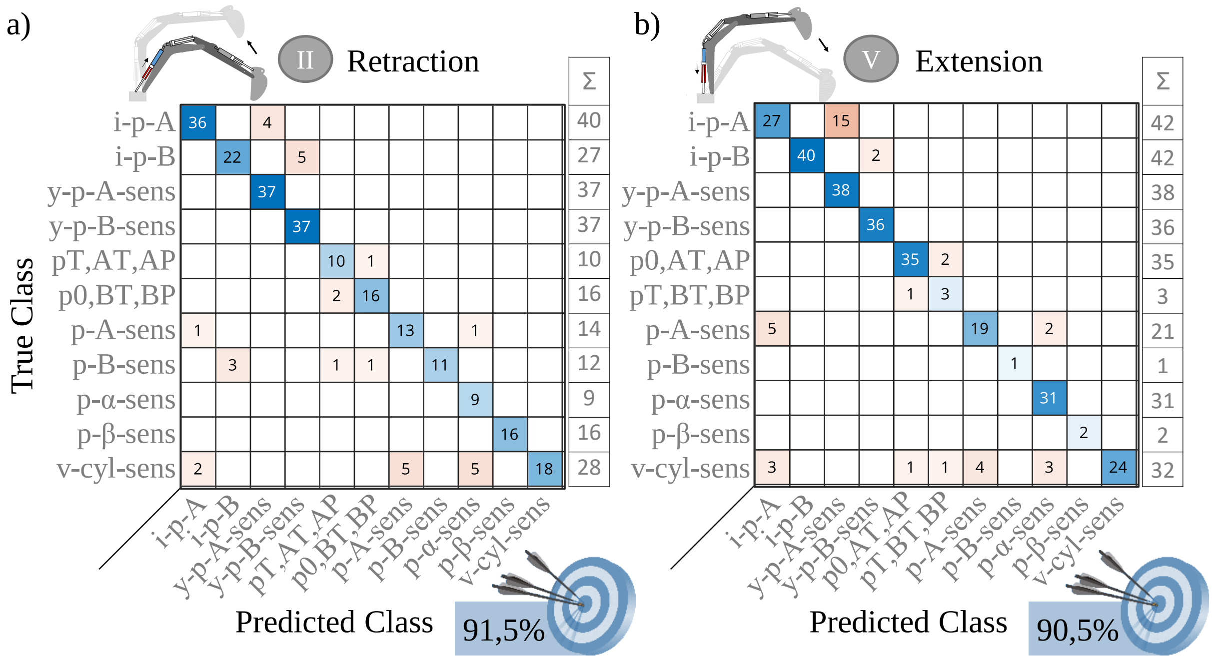

Figure 6: Confusion matrix for a) operating point II and b) operating point V with localization by means of Manhattan distance.

4.4. Fault localization via learning vector quantization

Learning vector quantization (LVQ) originates from the field of machine learning. Unlike the other three variants for fault localization, which follow a causal and analytical approach, LVQ cannot easily transfer its results to other system structures. For this reason, this approach will only be briefly discussed. LVQ is a prototype-based artificial neural network method for data classification. By an optimization, the choice of the prototype characteristics takes place in such a way that the associated data points have a minimum, class foreign a maximum distance to the prototype. An object is then classified according to the resulting Voronoi regions using the winner-takes-it-all principle. Consequently, only one fault class is assigned to each fault scenario. Numerous LVQ algorithms are available in literature. The "Generalised Relevance LVQ" algorithm described in [10], [11] was utilised in this work. This method optimizes the features of the prototypes as well as the weighting of the symptoms.

Despite the extensive variant study, only few training data sets are available, if one applies the standards of machine learning algorithms. Furthermore, there is no uniform distribution of failure scenarios, since some components have a binary fault character (e.g. switching valve is open or closed). As a result, the promising LVQ algorithm reaches its limits and only achieves classification accuracies within the range of 80%. In addition, there are the well-known challenges in the use of machine-learning algorithms, such as transferability of results and overfitting.

5. TESTING OF FAULT LOCALIZATION ON THE TEST BENCH

For fault localization on the test bench, the geometric classification method is implemented using the Manhattan distance. This consistently continues the knowledge-based approach of model-based fault detection and achieves the best localization accuracy in the simulation study. **Figure 7** shows the detected threshold exceedances as a result of a velocity sensor error. The first symptom is generated by parity equation A3 where the status changed from false “f” to true “t”. Other symptoms appear subsequently, mainly of equations A1, B1, A4, A5 and B5. If the movement of the boom ends at 10.5s, the permitted thresholds are no longer exceeded. The parity equations A1 and A4 are the last to fall below the thresholds.

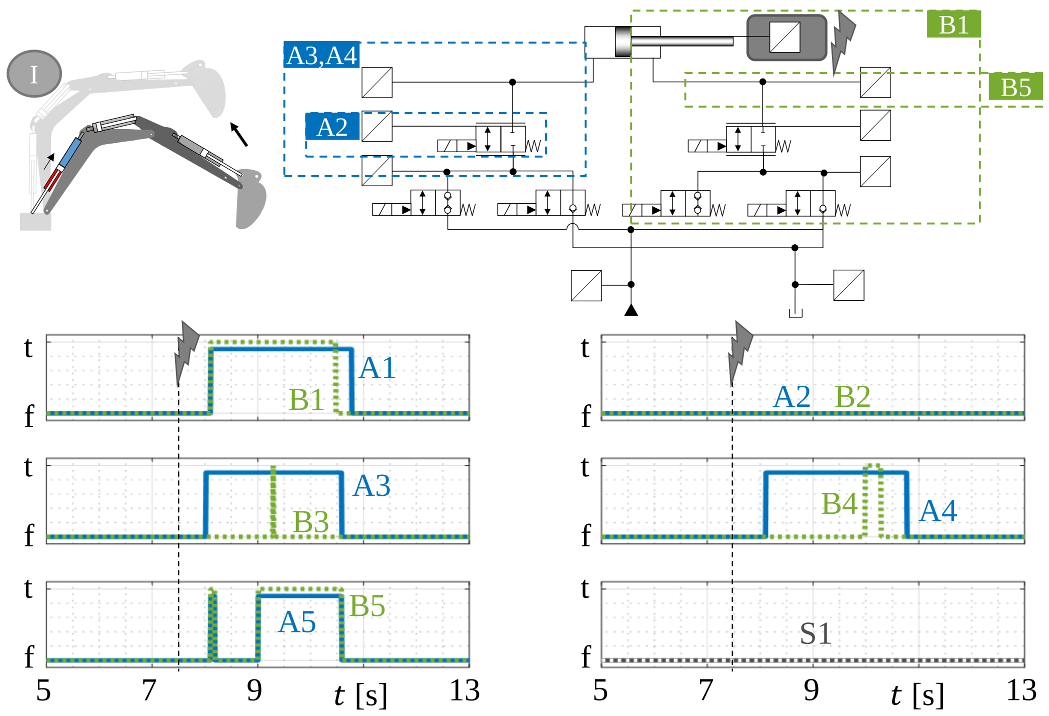

Figure 7: Currently detected threshold exceedances of all parity equations in case of a velocity sensor error at operating point I (measurement)

The fault cases are classified based on temporary threshold violations and corresponding symptoms.

Figure 8 clearly shows that the fault is mostly classified correctly during the movement phase (the classification marker "v-cyl-sens" changes from false to true), although there is no fully developed symptom pattern at any time (see Table 1). Only at the beginning and at the end of the movement the calculated Manhattan distance indicates another cause of error. Nevertheless, the measurement illustrates the effectiveness of fault localization and the validity of the simulatively obtained statements in an exemplary manner.

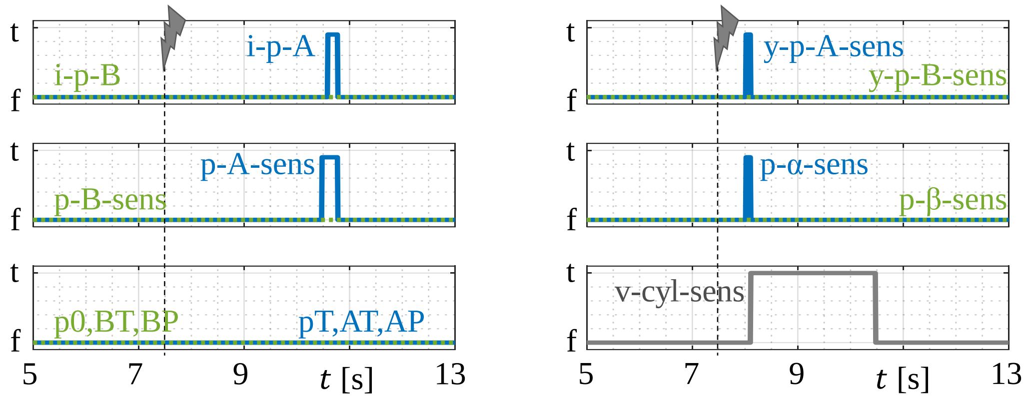

Figure 8: Resulting classification in case of a velocity sensor error at operating point I (measurement)

Another classification example is displayed in **Figure 9**, showing a malfunctioning rod-side pressure sensor p_β positioned between the proportional and switching valves. This sensor outputs the maximum value instead of the real pressure. The machine controller uses the wrong value for valve actuation, causing the proportional valve on the drain side to open too wide. The system cannot generate the necessary pressure to support the equipment, causing the boom to move too quickly towards the ground (see **Figure 10 a)**). This fault state is reliably detected by parity equations B3 and B4 and accurately localized by Manhattan distance.

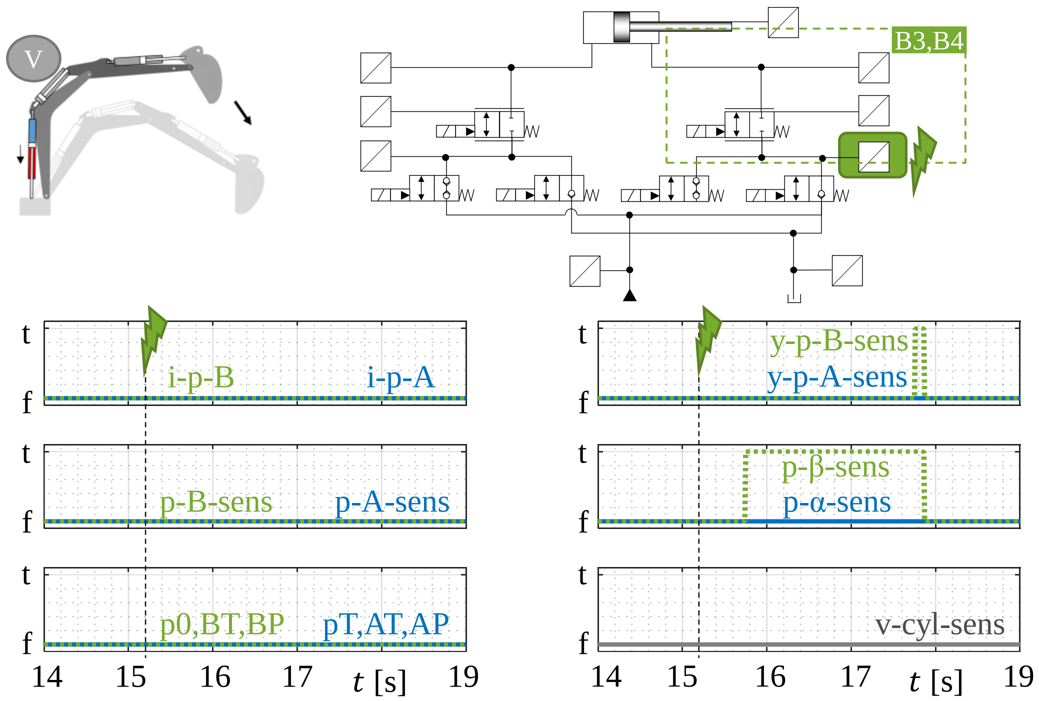

Figure 9: Classification of error “faulty value of sensor p_β (maximum value)” at operating point V.

In case of detecting a fault, appropriate responses can be taken to address the issue. One option is to close all valves and shut down the actuator completely. This is a safe option, but at the expense of availability. The correctly localized cause of error enables another option: reconfiguration.

Reconfiguration describes the upkeep of functionality in the case of failure, through compensating the faulty component. IM systems basically offer 2 possibilities for reconfiguration:

- mode switching
- alternative control strategies

Mode switching describes the structural compensation of a fault through alternative flow paths and is a characteristic of IM systems. However, the use of alternative control strategies is applicable to all appropriate systems. A key requirement for this compensation is usually an extensive sensory set-up. When a faulty sensor is identified, a control concept for valve actuation is chosen that does not rely on the faulty sensor value. The performance of both concepts can be demonstrated on the test rig. In the case of the sensor error p_β, the use of an alternative control strategy is suitable (see Figure 10 b)). After the error occurs, the fault cause is accurately identified (see Figure 9) and the control strategy is adjusted accordingly. The pressure drop over the proportional valve can no longer be determined directly due to the faulty sensor. By using the system pressures in the supply and tank lines and a combined resistance model of the switching and proportional valve, adequate valve control is nevertheless possible. This ensures that the cylinder's movement remains manageable, preventing hazardous movements as well as drive shutdown.

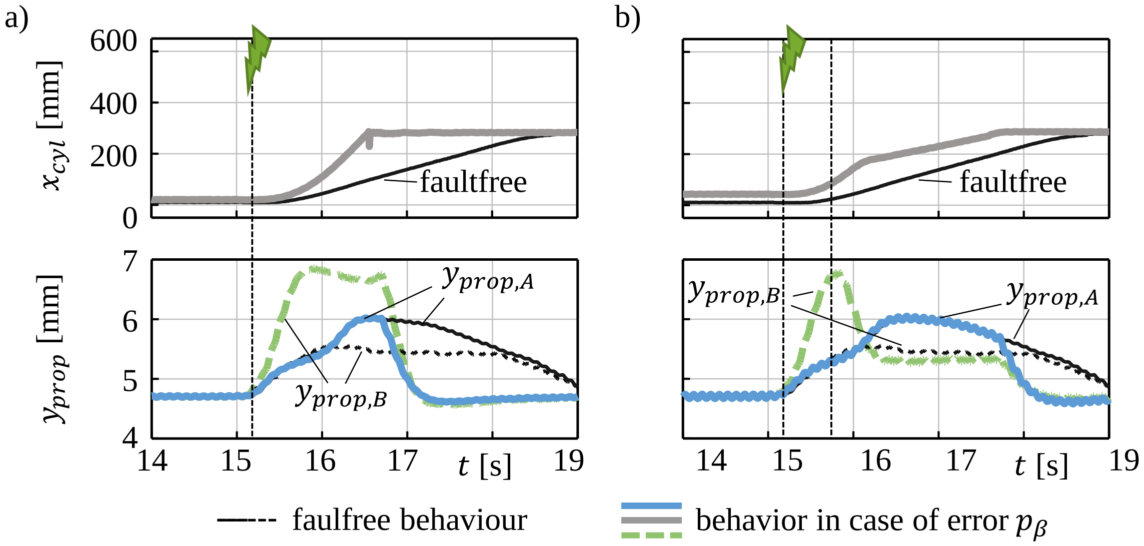

Figure 10: Measured behavior in case of error "faulty value of sensor p_β (maximum value)" a) without error detection and b) with error detection and reconfiguration at operating point V.

6. CONCLUSION AND OUTLOOK

The paper presents a model-based fault management for IM-systems. Fault detection and fault localization utilize existing system knowledge. The practical modelling approach employs a set of 11 parity equations for fault detection. The different balance limits of these equations generate selective symptoms for different fault scenarios. This is an essential prerequisite for identifying the specific fault cause.

Different approaches have been investigated for fault localization. In particular, localization based on Manhattan distance leads to promising results of up to 92% accuracy. This method can easily be transferred to other system structures. However, it turns out that an extension of the parity equation set could provide benefits. Particularly, descriptions of component-specific elements enhance the reliability of detection and increase depth of localization.

The reconfiguration of correctly localized faulty components can be successfully demonstrated. Depending on the fault and reconfiguration possibility, partial or even complete compensation is possible.

The transfer of the investigated algorithms to the real system allows the validation of the results. The exemplary verification leads to a good agreement with the results of the simulation study. The test rig results therefore confirm the theoretical analyses and conclusions.

7. ACKNOWLEDGEMENTS

The project "Adaptive modellbasierte Fehlererkennung und -diagnose mit rekonfigurierbaren elektrohydraulischen Systemen" (IGF 20246 BR/1) was financed and supervised by the Research Association Mechanical Engineering (FKM), Frankfurt am Main. In the scope of the program to promote Industrial Collective Research it was funded by the German Federation of Industrial Research Associations (AiF) with means of the Federal Ministry for Economic Affairs and Climate Action on the basis of a decision by the German Bundestag.

Supported by:

Federal Ministry
for Economic Affairs
and Climate Action

on the basis of a decision
by the German Bundestag

NOMENCLATURE

A1…A5	Parity equations or their symptoms on the piston side	
B1…B5	Parity equations or their symptoms on the rod side	
Δx_{cyl}	Deviation of the cylinder position due to an error	m
IM	Independent metering (system)	
r_{limit}	Threshold of the parity equation residuals	
S1	Parity equation S1 or its symptom	
t	Time	s
t/f	true/false	
$V_{prop,A/B}$	Proportional valve on the piston / rod side	
$V_{svBP/BT}$	Switching valve to connect the rod side with pump or reservoir	
$V_{svAP/AT}$	Switching valve to connect the piston side with pump or reservoir	
x_{cyl}	Cylinder position	mm
$\dot{x}_{cyl}$	Cylinder velocity	m/s
y/n	yes/no	
$y_{prop,A/B}$	Position of proportional valve $V_{prop,A/B}$	mm

REFERENCES

[1] Eaton (2016), Data Sheet, CMA200 Advanced Independent-Metering Mobile Valve. 2016

[2] Danfoss (2016), Data Sheet. Proportional Valve PVX. 2016

[3] Beck B., Weber J. (2016), Safety and Reliability of Independent Metering Systems in Mobile Machinery. In: 26th European Safety and Reliability Conference, ESREL 2016, Glasgow, Scotland, September 25-29, 2016,

[4] Fischer E., Beck B., Weber J. (2022), Data analysis for the evaluation and design of a model-based fault detection based on an independent metering system for mobile hydraulic drives. In: 13th International Fluid Power Conference, 13. IFK, Aachen, Germany, March 21-23, 2022

[5] Jansson A., Krus P., Palmberg J.-O. (1991), Decoupling of response and pressure level in a hydraulic actuator. In: Fluid power systems modelling and control. Fourth Bath International Fluid Power Workshop on Systems. Bath, UK, September 18-20, 1991

[6] Richter S. (2016), Ein Beitrag zur Integration von Maßnahmen der funktionalen Sicherheit in einen geregelten elektrohydraulischen Antrieb für stationäre Anwendungen. PhD thesis, TU Dresden, Shaker Verlag, Aachen, 2016

[7] Kramer T., Weber J. (2018) ,Intelligent Condition Monitoring of Bi-stable Process Valves. In: 11th International Fluid Power Conference, 11. IFK, Aachen, Germany, March 19-21, 2018

[8] Isermann R. (2006), Fault-Diagnosis Systems. An Introduction from Fault Detection to Fault Tolerance. Springer, Berlin Heidelberg, 2006

[9] Clauß G., Finze F.-R., Partzsch L. (1994), Statistik. Für Soziologen, Pädagogen, Psychologen und Mediziner. Band 1, Verlag Harri Deutsch, Thun, Frankfurt am Main, 1994

[10] Bunte K., Schneider P., Hammer B., et al. (2012), Limited Rank Matrix Learning - Discriminative Dimension Reduction and Visualization. In: Neural Networks, Volume 26, 2012

[11] Schneider P., Biehl M., Hammer B. (2009), Adaptive Relevance Matrices in Learning Vector Quantization. In: Neural Computation, Volume 21, 2009